REGULAR ARTICLE

Proteomic dataset of Sca-1$^+$ progenitor cells

Xiaoke Yin[1], Manuel Mayr[1], Qingzhong Xiao[1], Ursula Mayr[1], Edward Tarelli[2], Robin Wait[3], Wen Wang[4] and Qingbo Xu[1]

[1] Department of Cardiac and Vascular Sciences, St. George's, University of London, London, UK
[2] Medical Biomics Centre, St. George's, University of London, London, UK
[3] Kennedy Institute of Rheumatology Division, Imperial College London, London, UK
[4] Medical Engineering Division, Department of Engineering, Queen Mary, University of London, London, UK

Embryonic stem cells (ES cells) can differentiate into endothelial cells and smooth muscle cells (SMCs), which participate in vascular angiogenesis. In this study, we differentiated mouse ES cells into Sca-1$^+$ cells, which have the potential to serve as vascular progenitor cells, and mapped their proteome by 2-DE using a pH 3–10 non-linear gradient and 12% SDS-polyacrylamide gels. A subset of 300 protein spots was analysed and mapped, with 241 protein spots being identified by their PMF using MALDI-TOF MS or by partial amino acid sequencing using MS/MS. Our protein map is the first of Sca-1$^+$ progenitor cells and will facilitate the identification of proteins differentially expressed during stem cell differentiation. The proteome of adult arterial SMCs is described in an accompanying paper (in this issue, DOI 10.1002/pmic.200402045). All data are made accessible on our website http://www.vascular-proteomics.com.

1 Introduction

Stem cells represent currently one of the most promising areas in medical research. Their totipotency and self-renewal capacity makes them a promising source for regeneration medicine [1]. It has been reported that embryonic stem cells (ES cells) can differentiate into cardiomyocytes [2], hemato-poietic progenitor cells [2], endothelial cells [3], skeletal and smooth muscle cells (SMCs) [4, 5], and several other tissue types [6–13]. However, the mechanisms of cell differentiation toward a specific direction and the protein changes involved are not fully elucidated yet.

A number of studies demonstrated that vascular progenitor cells, including endothelial and smooth muscle progenitors, are present in circulating blood and have the capacity to differentiate into mature SMCs and endothelial cells [14–19], thereby contributing to vascular repair, remodeling, and atherosclerotic lesion formation [18, 20–22]. Recently, we have provided evidence that both endothelial cells and SMCs in atherosclerotic lesions and neointima in mice are derived from stem/progenitor cells [23–25]. Thus, vascular progenitor cells play an important role in pathophysiology of the vessel wall as well as angiogenesis.

There is evidence indicating that Flk-1$^+$ progenitor cells can differentiate into both endothelial cells and SMCs in response to VEGF and PDGF-BB stimulation, respectively [26, 27]. A recent report from our laboratory demonstrated that stem cell antigen-1-positive (Sca-1$^+$) cells isolated from adventitial tissues can differentiate into SMCs [28]. In the present study, we induced ES cell differentiation and isolated Sca-1$^+$ cells, which may serve as vascular progenitor cells. We studied their proteome by 2-DE, and created a reference protein map of Sca-1$^+$ progenitor cells that will be useful for studying protein alterations during cell differentiation.

Correspondence: Prof. Qingbo Xu, Department of Cardiac and Vascular Sciences, St. George's, University of London, Cranmer Terrace, London, SW17 0RE, UK
E-mail: q.xu@sgul.ac.uk
Fax: +44-208-725-2812

Abbreviations: ES cell, embryonic stem cell; **DM**, differentiation medium; **Flk-1**, foetal liver kinase-1; **LIF**, leukaemia inhibitory factor; **MACS**, magnetic-activated cell sorting; **PDGF**, platelet-derived growth factor; **Sca-1**, stem cell antigen-1; **SMC**, smooth muscle cell; **SSEA-1**, stage specific embryonic antigen-1; **VEGF**, vascular endothelial growth factor

2   Materials and methods

2.1 Mouse ES cells culture

Mouse ES cells (ES-D3 cell line, CRL-1934, ATCC) were maintained as described previously [29]. Briefly, ES cells were cultured in DMEM (ATCC) containing 10 ng/mL recombinant human leukaemia inhibitory factor (LIF, Chemicon), 10% foetal bovine serum (FBS, ATCC), 0.1 mM 2-mercaptoethanol (Sigma), 2 mM L-glutamine (Invitrogen), 100 U/mL penicillin (Invitrogen), and 100 µg/mL streptomycin (Invitrogen). Undifferentiated ES cells were passaged into flasks coated with 0.04% gelatin (Sigma) at a ratio of 1:6 to 1:10 every 2 days.

2.2 Differentiation of ES cells

ES-D3 cells were cultured on type IV mouse collagen (Trevigen) coated flasks for 3–4 days in basic differentiation medium (DM): alpha-minimal essential medium (α-MEM, Invitrogen), supplemented with 10% foetal calf serum (FCS, Invitrogen) and 50 µM 2-mercaptoethanol. Sca-1$^+$ cells were sorted from the cell culture by magnetic-activated cell sorting (MACS) with anti-Sca-1 microbeads (Miltenyi Biotec) as described in our previous studies [28]. Briefly, cells were detached with trypsin-EDTA solution (Invitrogen) from flasks and incubated with the antibody-conjugated/coated microbeads. With occasional agitation for 15 min at 4°C, the bead-bound cells were selected using a magnetic cell separator (Miltenyi Biotec). Sca-1$^+$ cells were resuspended in fresh DM and passaged every 2 days. Cells were harvested for 2-DE after ten passages.

2.3 Haematoxylin and eosin staining

Cells were plated in 8-well chamber slides (Nalge Nunc) and cultured in ES cell culture medium or basic DM for 3 days then fixed and stained with Haematoxylin and eosin (H&E).

2.4 RT-PCR

Total RNA of ES cells and Sca-1$^+$ progenitor cells were extracted using RNeasy kit (Qiagen). RNA was quantified with a UV spectrophotometer and cDNA was synthesized from 2.5 µg total RNA for each reverse transcription reaction. Reverse transcription was performed using Improm-II™ RT kit (Promega) with RNase inhibitor (Promega) and random primers (Promega). Control reverse transcription reactions were performed without reverse transcriptase. PCR was performed using a PCR kit (Invitrogen) with 50 ng cDNA. Primer sequences were as follows: Sca-1: forward: 5'-TCT GAG GAT GGA CAC TTC TC-3', reverse: 5'-CTC AGG CTG AAC AGA AGC AC-3'; GAPDH: forward: 5'-CGG AGT CAA CGG ATT TGG TCG TAT-3', reverse: 5'-AGC CTT CTC CAT GGT GGT GAA GAC-3'.

2.5 Immunofluorescence staining

The procedure was similar to that described previously [28]. Briefly, cultured cells were labelled with mouse monoclonal antibodies to stage-specific embryonic antigen-1 (SSEA-1; clone MC-480; Chemicon) and Sca-1 (clone E-13-161.7; BD biosciences), and visualized with rabbit anti-mouse immunoglobulin conjugated with fluorescein isothiocyanate (FITC; DAKO Cytomation) or phycoerythrin (PE; DAKO). 4',6-diamidino-2-phenylindole (DAPI; Sigma) was used for counterstaining. Cells were mounted in Floromount-G (DAKO) and examined under a fluorescence microscope (Zeiss).

2.6 Flow cytometry analysis

The procedure was similar to that described previously [28]. Briefly, cultured cells were incubated with dissociation buffer (Invitrogen) for 3 min and blocked with diluted serum (the species of serum is the same as that for the secondary antibody) for 20 min on ice. The single-cell suspension was aliquoted and incubated with either isotype control or SSEA-1 and Sca-1 antibodies for 30 min on ice, then incubated with rabbit anti-mouse or anti-rat immunoglobulin conjugated with FITC. Cell suspensions were analysed with FACScan (Becton Dickinson Immunocytometry Systems). Data analysis was carried out using CellQuest software (Becton Dickinson).

2.7 2-DE

The protocol used for proteomic analysis is similar to that described before [30, 31]. Cells were scraped and centrifuged at 4°C, 13.2 krpm, for 1 min. Cell pellets were lysed in 2-DE lysis buffer (9.5 M urea, 2% CHAPS, 0.8% pharmalyte, pH 3–10 and 1% DTT) for 30 min, and centrifuged for 20 min at 20°C, 13.2 krpm. The supernatant was divided into aliquots and protein concentration was determined. Extracts were diluted directly with rehydration solution (8 M urea, 0.5% CHAPS, 0.2% DTT, and 0.2% pharmalyte pH 3–10) or subject to an additional clean-up procedure using 2-D Prep-Ready CleanUp Kit (Bio-Rad) to remove contaminants interfering with IEF. Protein samples were loaded on 18-cm non-linear immobilized pH gradient strips, pH 3–10 (Immobiline DryStrips, GE Healthcare); 100 µg total protein was used for analytical gels and 400 µg for preparative gels. After overnight rehydration, strips were focused in Multiphor™ II IEF System (GE Healthcare) at 0.05 mA/IPG strip for 60 kVh at 20°C. Once IEF was finished, the strips were equilibrated in equilibration buffer (6 M urea, 30% glycerol, 2% SDS and 0.01% bromophenol blue) with addition of 1% DTT for 15 min, followed by a further 15 min equilibration in the same buffer containing 4.8% iodoacetamide in place of DTT. SDS-PAGE was performed using 12%T, 2.6% C polyacrylamide gels without a stacking gel and the Ettan™ DALTsix vertical electrophoresis system (GE Healthcare). The second dimension was carried out at 10°C until the bromophenol

blue dye front had migrated off the lower end of the gels. Gels were stained by silver staining (PlusOne™ Silver Staining Kit, Protein, GE Healthcare) using a slightly modified protocol [32], which is compatible with MS. Spots were detected, matched, and overlaid to create difference maps using the ProteomWeaver software (Definiens).

2.8 MALDI-TOF MS

Silver-stained spots were picked and treated overnight with sequencing grade modified trypsin (Promega) according to a published protocol [33]. Peptide fragments were recovered by sequential extractions with 100 mM ammonium bicarbonate and extraction solution (5% formic acid, 50% ACN). Extracts were lyophilised, resuspended in 10 µL 0.1% TFA, and desalted with µC-18 ZipTip (Millipore) according to the manufacturer's instruction. MALDI-TOF MS was performed using an Axima CFR spectrometer (Kratos). The instrument was operated in the positive ion reflectron mode, and 1 µL sample and 1 µL matrix (10 mg CHCA in 300 µL 0.1% TFA and 700 µL ACN) were applied. Spectra were internally calibrated using trypsin autolysis products. Peaks were labelled and their peptide masses were used to search against databases using the MASCOT program [34]. One missed cleavage per peptide was allowed and carbamidomethylation of cysteine as well as partial oxidation of methionine were assumed.

2.9 Q-TOF MS/MS

In-gel digestion with trypsin was performed according to published methods [32–35] modified for use with an Investigator ProGest (Genomic Solutions) robotic digestion system. Mass spectra were recorded using a Q-TOF mass spectrometer (Micromass) interfaced to a Micromass CapLC capillary chromatograph. Samples were dissolved in 0.1% aqueous formic acid, injected onto a 300 µm × 5 mm Pepmap C18 column (LC Packings), and eluted with an ACN/0.1% formic acid gradient. The capillary voltage was set to 3500 V, and data-dependent MS/MS acquisitions were performed on precursors with charge states of 2, 3, or 4 over a survey mass range of 540–1000. The collision gas was argon, and the collision voltage was varied between 18 and 45 V depending on the charge-state and mass of the precursor. Initial protein identifications were made by correlation of uninterpreted tandem mass spectra to entries in Swiss-Prot and TREMBL, using ProteinLynx Global Server (V 1.1, Micromass).

2.10 LCQ IT MS/MS

Following enzymatic degradation, peptides were separated by capillary LC on a reverse-phase column (BioBasic-18, 100 × 0.18 mm, particle size 5 µm, Thermo Electron Corporation) and applied to a LCQ IT mass spectrometer (Finnigan LCQ Deca XP Plus, Thermo Electron Corporation) interfaced with a Finnigan Surveyor autosampler (Thermo Electron Corporation). The peptides were eluted using an ACN/0.1% formic acid gradient. Spectra were collected from the IT mass analyser using full ion scan mode over the *m/z* range 300–2000. MS/MS scans were performed on each ion using dynamic exclusion. Database search was performed using TurboSEQUEST program (BioWorks Browser v3.1, Thermo Electron Corporation).

3 Results

Sca-1$^+$ cells were isolated from ES cells with microbeads and cultivated on gelatin-coated plates. Their phenotype was verified using H&E and immunofluorescence staining, RT-PCR and FACS analysis (Fig. 1). Morphologically, Sca-1$^+$ progenitor cells displayed a monolayer in culture, while ES cells showed clusters in an undifferentiated status for more than 35 passages in our culture conditions (Fig. 1A). Transcription of Sca-1 was significantly increased in Sca-1$^+$ progenitor cells compared to ES cells, as verified by RT-PCR (Fig. 1B). While
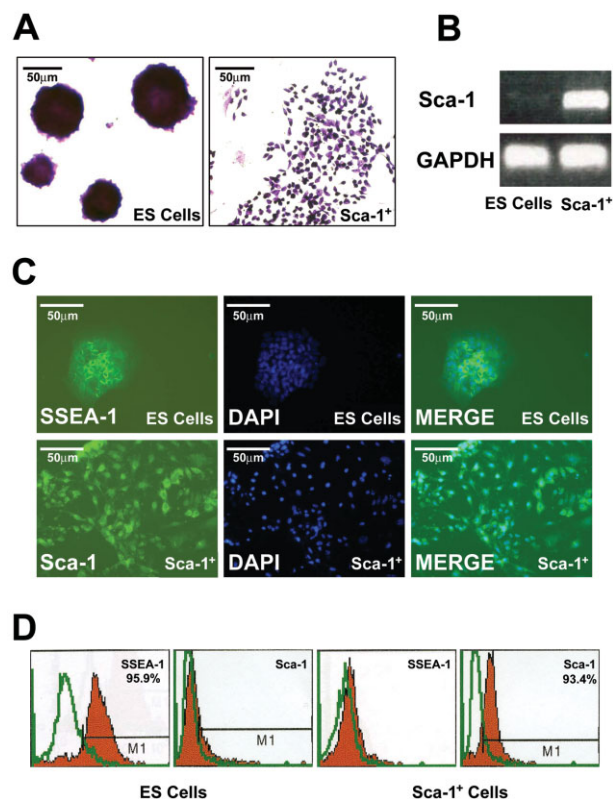
Figure 1. The morphology and characteristics of ES cell-derived Sca-1$^+$ progenitor cells. (A) ES cells and Sca-1$^+$ progenitor cells were stained by H&E. (B) mRNA levels of Sca-1 were quantified by RT-PCR in ES cells and Sca-1$^+$ progenitor cells. GAPDH was included as a loading control. (C) SSEA-1 and Sca-1 were detected by immunofluorescence staining. Nuclei were counterstained with DAPI, shown in blue. (D) For flow cytometry, cells were dissociated and incubated with either isotype control (green line) or antibodies to SSEA-1 for ES cells and antibodies to Sca-1 for Sca-1$^+$ progenitor cells (red line), respectively.
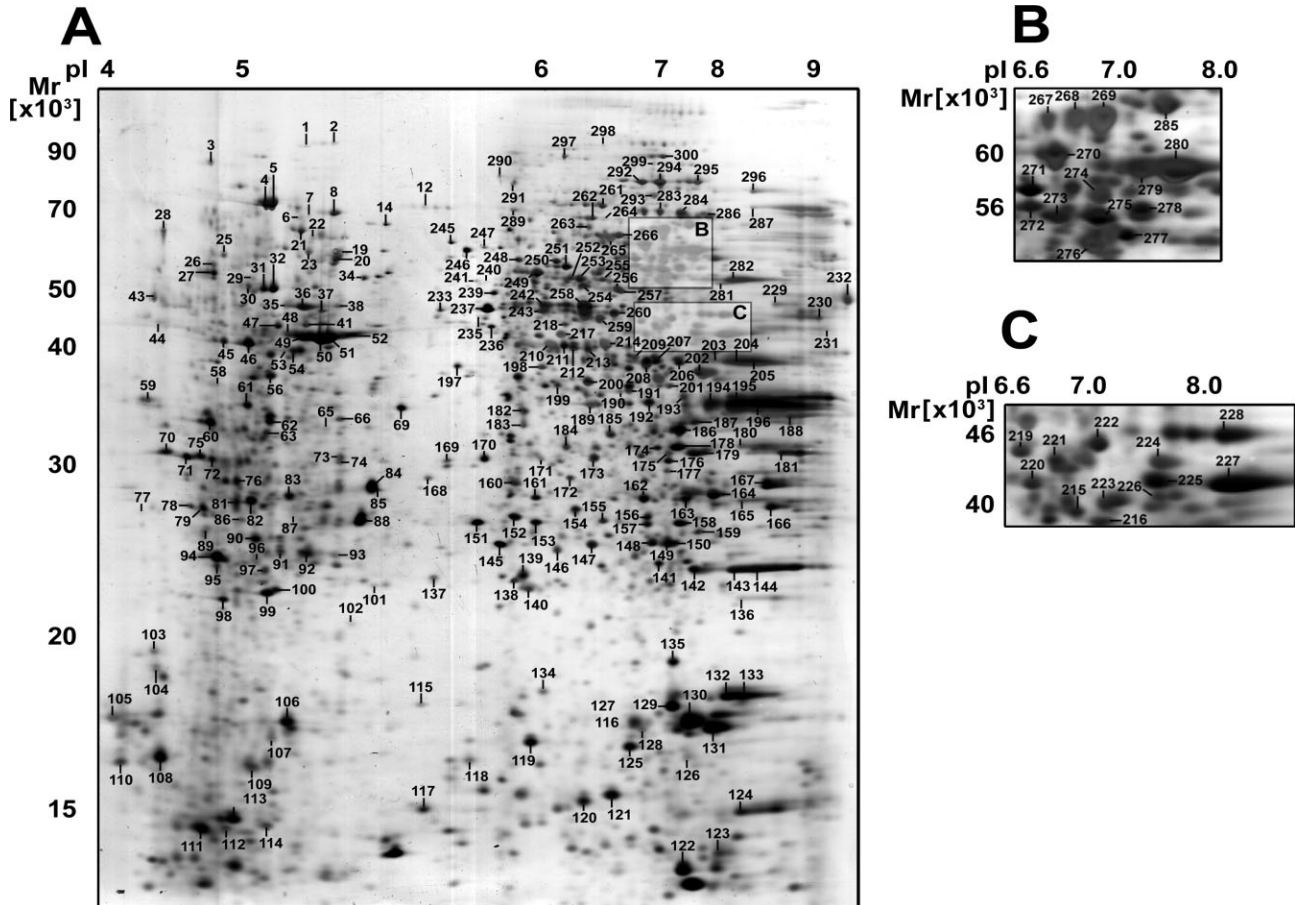
Figure 2. Proteome map of Sca-1$^+$ progenitor cells. Protein extract (400 μg) was separated on a pH 3–10NL IPG strip, followed by SDS-PAGE on a 12% gel. (A) Protein spots were visualized by silver staining. Labelled spots were picked for protein identification. The highlighted areas are enlarged in inset B and C.

SSEA-1 was expressed in ES cells, Sca-1 was detected only in Sca-1$^+$ progenitor cells by immunofluorescence staining (Fig. 1C). Flow cytometry revealed that 95.9% of ES cells, but none of the Sca-1$^+$ progenitor cells stained positive for SSEA-1. In contrast, Sca-1 was detectable in 93.4% of Sca-1$^+$ progenitor cells but not in ES cells (Fig. 1D). Taken together, these results confirm the high homogeneity of the Sca-1$^+$ progenitor cell population.

Subsequently, proteins of Sca-1$^+$ progenitor cells were harvested for 2-DE. Protein samples were separated before and after using a clean-up kit (Bio-Rad) (Figs. 2 and 3, respectively). Overall, the spot pattern was very similar and the clean-up procedure prevented streaking in the basic area. However, some spots disappeared after using the clean-up kit, mainly in the basic region (pI >8) and in the lower left corner of the gel (spots 44, 73, 74, 81, 85, 89, 109, 144, 166, 175, 181, 188, 190, 224, 230–232), while additional spots became detectable in the treated sample (spots 9–11, 13, 15–18, 24, 33, 39, 40, 42, 55, 57, 64, 67, 68, 80, 116, 234, 238, 244, 288).

From approximately 2000 spots that were resolved on a single large format silver-stained gel, 300 were picked for MS

(Figs. 2, 3). Of these, 241 spots were identified representing 172 unique proteins with a molecular mass range from 10 to 100 kDa and a pI range from 4 to 9. Fifty-nine spots (19.7%) remained unidentified. All identifications are listed in Table 1 and can be found on our website: http://www.vascular-proteomics.com.

The majority of proteins were enzymes (36.6%), followed by proteins involved in DNA maintenance, transcription, translation (19.8%), structural proteins (10.5%) and chaperones (14.5%). A direct comparison revealed that signalling molecules were more abundant in Sca-1$^+$ progenitor cells (12.2%) than adult arterial SMCs [36]. Overall, the percentage of differentially expressed spots (twofold increased or decreased) was higher between arterial SMCs and Sca-1$^+$ progenitor cells than between Sca-1$^+$ progenitor cells and ES cells, indicating that the proteome of Sca-1$^+$ progenitor cells remained more similar to ES cells than differentiated mature SMCs (Fig. 4). Using the link "SEARCH SPOTS" on our website, proteins can be listed according to their categories and compared between the different cell lines.

Figure 3. Proteome map of Sca-1⁺ progenitor cells after using a clean-up kit. Protein extract (400 μg) was treated with a clean-up kit and separated on a pH 3–10NL IPG strip, followed by SDS-PAGE on a 12% gel. (A) Protein spots were visualized by silver staining. Labelled spots were picked for protein identification. The highlighted areas are enlarged in inset B and C.
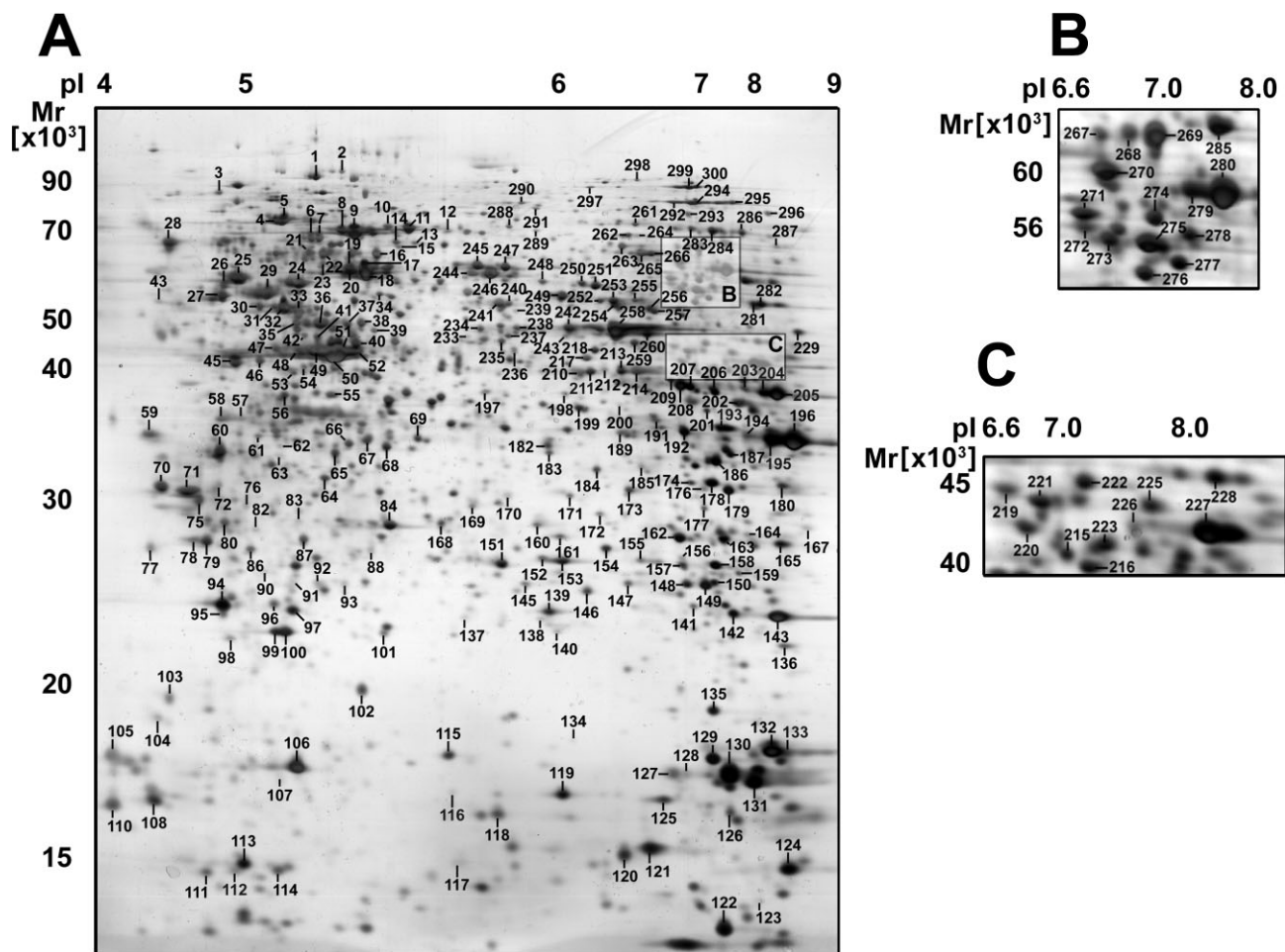
4 Discussion

In the present study, we utilized the potential of proteomic techniques and made a first attempt to clarify protein changes during stem cell differentiation to SMCs. The remarkable differentiation potential of stem cells holds important research applications including neoangiogenesis, stem cell-based therapies and tissue-engineering strategies, which may offer new clinical applications.

Stem cell differentiation is a complex process altering numerous proteins, not only at the transcriptional and translational level, but also by post-translational modification. The comprehensive approach of proteomic techniques will allow us to get a better understanding of stem/progenitor cells differentiation *in vitro* and *in vivo*. However, before we can analyse protein differences in detail, reliable and applicable reference maps of each differentiation stage must be established. To date, a protein map of murine ES cells has been published by Elliott *et al.* [37]. Here we describe the proteome

of Sca-1⁺ progenitor cells, the early differentiation step from ES cells to SMCs. The proteome of differentiated mature SMCs has been analysed in a sister paper [36].

Compared with Sca-1⁺ progenitor cells, the expression of myofilaments and associated proteins, such as actin, myosin light chain, tropomyosin and calcium-binding proteins (calcyclin, calpactin I light chain, transgelin), is higher in SMCs. In contrast, proteins related to DNA maintenance, transcription and translation show decreased expression in SMCs compared to Sca-1⁺ progenitor cells, *e.g.*, heterogeneous nuclear ribonucleoprotein, translation initiation factor, elongation factor, translationally controlled tumour protein. Other differences in signalling proteins such as Rho GDP-dissociation inhibitor 1, an endogenous inhibitor of Rho signalling pathways, which was associated with cytoskeletal abnormalities and phenotypic modulation in PKCδ-deficient SMCs [38], may implicate certain receptors and signalling pathways in regulating stem cell differentiation.

Table 1. Protein list of Sca-1^{+} progenitor cells

ID	Protein name	Swiss-Prot entry name	Swiss-Prot accession no.	Calculated MW Da (×10³)/p*I*	Observed MW Da (×10³)/p*I*	Sequence coverage %	MASCOT Score
1	Heat shock protein 4	Q99L75_MOUSE	Q99L75	94.1/5.1	94.0/5.1	24	155
2	Caspase-8 [Precursor]	CASP8_MOUSE	O89110	55.4/5.1	94.1/5.3	15	68
3	Endoplasmin [Precursor]	ENPL_MOUSE	P08113	92.5/4.7	83.9/4.8	19	123
4	78-kDa glucose-regulated protein [Precursor]	GRP78_MOUSE	P20029	72.4/5.1	72.4/5.1	34	237
5	78-kDa glucose-regulated protein [Precursor]	GRP78_MOUSE	P20029	72.4/5.1	72.3/5.1	16	92
6	Lamin B1	LAM1_MOUSE	P14733	66.7/5.1	66.5/5.1	28	142
7	Lamin B1	LAM1_MOUSE	P14733	66.7/5.1	66.7/5.1	33	191
8	Heat shock cognate 71-kDa protein	HSP7C_MOUSE	P63017	70.9/5.4	70.9/5.3	24	136
9	Heat shock cognate 71-kDa protein	HSP7C_MOUSE	P63017	70.9/5.4	70.8/5.4	30	150
10	Stress-70 protein, mitochondrial [Precursor]	GRP75_MOUSE	P38647	73.5/5.9	71.3/5.4	14.43[a]	8[b]
11	Stress-70 protein, mitochondrial [Precursor]	GRP75_MOUSE	P38647	73.5/5.9	71.3/5.5	35	312
12	Rho-associated protein kinase 2	ROCK2_MOUSE	P70336	160.6/5.7	68.4/5.6	10	72
13	Stress-70 protein, mitochondrial [Precursor]	GRP75_MOUSE	P38647	73.5/5.9	65.1/5.5	15	72
14	Heat shock cognate 71-kDa protein	HSP7C_MOUSE	P63017	70.9/5.4	64.7/5.5	25	132
15	Stress-70 protein, mitochondrial [Precursor]	GRP75_MOUSE	P38647	73.5/5.9	63.5/5.5	16	107
16	Heterogeneous nuclear ribonucleoprotein K	HNRPK_MOUSE	P61979	51.0/5.4	62.2/5.4	25	121
17	60-kDa heat shock protein, mitochondrial [Precursor]	CH60_MOUSE	P63038	61.0/5.9	59.6/5.4	22	115
18	60-kDa heat shock protein, mitochondrial [Precursor]	CH60_MOUSE	P63038	61.0/5.9	59.6/5.4	22	94
19	Lamin B1	LAM1_MOUSE	P14733	66.7/5.1	58.8/5.4	18.20[a]	9[b]
20	Unidentified	–	–	–	58.0/5.3	–	–
21	78-kDa glucose-regulated protein [Precursor]	GRP78_MOUSE	P20029	72.4/5.1	64.3/5.1	31.30[a]	17[b]
22	Heterogeneous nuclear ribonucleoprotein K	HNRPK_MOUSE	P61979	51.0/5.4	61.6/5.2	20	92
23	Stress-70 protein, mitochondrial [Precursor]	GRP75_MOUSE	P38647	73.5/5.9	59.7/5.1	13	104
24	Vimentin	VIME_MOUSE	P20152	53.6/5.1	56.9/5.1	26	104
25	Protein disulfide isomerase [Precursor]	PDIA1_MOUSE	P09103	57.1/4.8	58.1/4.9	27	203
26	Endoplasmin [Precursor]	ENPL_MOUSE	P08113	92.5/4.7	55.5/4.8	23.94[a]	17[b]
27	Chromatin assembly factor 1 subunit C	RBBP4_MOUSE	Q60972	51.8/5.0	55.0/4.8	22.77[a]	7[b]
28	Calreticulin [Precursor]	CRTC_MOUSE	P14211	48.0/4.3	61.1/4.5	20	94
29	Tubulin beta-5 chain	TBB5_MOUSE	P05218	49.7/4.8	54.6/5.1	27	110
30	Histone acetyltransferase type B subunit 2	RBBP7_MOUSE	Q60973	47.8/4.9	52.9/5.1	19	85
31	ATP synthase beta chain, mitochondrial [Precursor]	ATPB_MOUSE	P56480	56.3/5.2	52.6/5.1	49.34[a]	18[b]
32	ATP synthase beta chain, mitochondrial [Precursor]	ATPB_MOUSE	P56480	56.3/5.2	52.6/5.1	32	161
33	Protein disulfide-isomerase A6 [Precursor]	PDIA6_MOUSE	Q922R8	48.1/5.0	51.4/5.1	22	96
34	Unidentified	–	–	–	54.1/5.4	–	–
35	26S protease regulatory subunit 6B	PRS6B_MOUSE	P54775	47.3/5.2	49.8/5.1	27	120
36	Heterogeneous nuclear ribonucleoprotein F	Q9Z2X1_MOUSE	Q9Z2X1	45.7/5.3	49.4/5.2	28	118
37	Eukaryotic translation initiation factor 3 subunit 5	IF35_MOUSE	Q9DCH4	38.0/5.3	48.4/5.3	19	91
38	Unidentified	–	–	–	49.1/5.4	–	–
39	Ubiquinol-cytochrome C reductase complex core protein I, mitochondrial [Precursor]	UQCR1_MOUSE	Q9CZ13	52.8/5.8	47.6/5.4	22.92[a]	8[b]
40	Similar to RIKEN cDNA 4921537P18	–	gi|51706188[c]	39.3/6.2	45.6/5.3	28	66
41	Thioredoxin domain containing protein 5 [Precursor]	TXND5_MOUSE	Q91W90	46.4/5.5	45.7/5.1	10.55[a]	3[b]
42	Vimentin	VIME_MOUSE	P20152	53.6/5.1	46.1/5.1	2.15[a]	1[b]
43	Calreticulin [Precursor]	CRTC_MOUSE	P14211	48.0/4.3	48.4/4.4	18.51[a]	4[b]
44	SET protein	SET_MOUSE	Q9EQU5	33.4/4.2	42.2/4.5	22	83
45	40S ribosomal protein SA	RSSA_MOUSE	P14206	32.6/4.7	40.4/4.9	30	70
46	Heat shock cognate 71-kDa protein	HSP7C_MOUSE	P63017	70.9/5.4	40.7/5.1	18	64
47	ATP synthase beta chain, mitochondrial [Precursor]	ATPB_MOUSE	P56480	56.3/5.2	44.7/5.1	35.73[a]	13[b]

Table 1. Continued

ID	Protein name	Swiss-Prot entry name	Swiss-Prot accession no.	Calculated MW Da ($\times10^3$)/pI	Observed MW Da ($\times10^3$)/pI	Sequence coverage %	MASCOT Score
48	Vimentin	VIME_MOUSE	P20152	53.6/5.1	42.5/5.1	4.95[a]	2[b]
49	Actin, cytoplasmic 1	ACTB_MOUSE	P60710	41.7/5.3	42.0/5.1	27	120
50	Actin, cytoplasmic 2	ACTG_MOUSE	P63260	41.8/5.3	41.6/5.2	29	124
51	Actin, cytoplasmic 1	ACTB_MOUSE	P60710	41.7/5.3	41.9/5.3	25	100
52	Actin, cytoplasmic 1	ACTB_MOUSE	P60710	41.7/5.4	41.7/5.4	4.2[a]	1[b]
53	Protein disulfide isomerase [Precursor]	PDIA1_MOUSE	P09103	57.1/4.8	39.8/5.1	5.31[a]	2[b]
54	Actin, cytoplasmic 1	ACTB_MOUSE	P60710	41.7/5.3	40.1/5.1	18	85
55	Suppressor of G2 allele of SKP1 homolog	SUGT1_MOUSE	Q9CX34	38.2/5.3	37.2/5.2	29	114
56	Hyaluronan mediated motility receptor	HMMR_MOUSE	Q00547	91.8/5.5	36.5/5.1	13	68
57	Nucleophosmin	NPM_MOUSE	Q61937	32.6/4.6	35.5/5.0	23	111
58	Nucleophosmin	NPM_MOUSE	Q61937	32.6/4.6	35.4/4.9	12.33[a]	3[b]
59	Nascent polypeptide-associated complex alpha subunit	NACA_MOUSE	Q60817	23.4/4.5	33.5/4.4	30	91
60	Proliferating cell nuclear antigen	PCNA_MOUSE	P17918	28.8/4.7	32.1/4.8	27	95
61	Unidentified	–	–	–	33.4/5.1	–	–
62	60-kDa heat shock protein, mitochondrial [Precursor]	CH60_MOUSE	P63038	61.0/5.9	32.5/5.1	20	70
63	Unidentified	–	–	–	32.0/5.1	–	–
64	Tropomyosin beta chain	TPM2_MOUSE	P58774	32.8/4.7	31.7/5.2	15	67
65	Ribosome biogenesis regulatory protein homolog	RRS1_MOUSE	Q9CYH6	41.6/10.8	32.1/5.2	30	62
66	Inorganic pyrophosphatase	IPYR_MOUSE	Q9D819	32.7/5.4	32.7/5.3	25	86
67	Tubulin beta-5 chain	TBB5_MOUSE	P05218	49.7/4.8	32.8/5.4	20	105
68	Pyruvate dehydrogenase E1 component beta subunit, mitochondrial [Precursor]	ODPB_MOUSE	Q9D051	38.9/6.4	32.3/5.5	33	91
69	Pyruvate kinase, isozyme M2	KPYM_MOUSE	P52480	57.8/7.4	32.8/5.5	4.33[a]	2[b]
70	Unidentified	–	–	–	30.9/4.5	–	–
71	Elongation factor 1-beta	EF1B_MOUSE	O70251	24.6/4.5	30.7/4.7	29	87
72	Tropomyosin 3, gamma	Q8K0Z5_MOUSE	Q8K0Z5	33.1/4.7	30.9/4.8	14.11[a]	3[b]
73	Actin, cytoplasmic 1	ACTB_MOUSE	P60710	41.8/5.3	31.0/5.3	13.83[a]	4[b]
74	Actin, cytoplasmic 1	ACTB_MOUSE	P60710	41.8/5.3	30.9/5.3	9.04[a]	3[b]
75	Tyrosine 3-monooxygenase / tryptophan 5-monooxygenase activation protein, epsilon polypeptide	Q8BPH1_MOUSE	Q8BPH1	29.2/4.6	29.4/4.7	36	114
76	Tumour necrosis factor receptor superfamily member 5 [Precursor]	TNR5_MOUSE	P27512	32.1/6.3	28.9/5.0	26	72
77	HIRA-interacting protein 5	HIRP5_MOUSE	Q9QZ23	22.1/4.2	25.9/4.4	26.13[a]	4[b]
78	Unidentified	–	–	–	26.5/4.7	–	–
79	Proteasome subunit alpha type 5	PSA5_MOUSE	Q9Z2U1	26.4/4.7	26.6/4.8	40	115
80	Unidentified	–	–	–	27.8/4.9	–	–
81	Unidentified	–	–	–	27.2/5.0	–	–
82	Unidentified	–	–	–	27.6/5.1	–	–
83	Unidentified	–	–	–	27.8/5.1	–	–
84	Actin, cytoplasmic 2	ACTG_MOUSE	P63260	41.8/5.3	28.1/5.4	16	68
85	Prohibitin	PHB_MOUSE	P67778	29.8/5.6	27.6/5.5	38	87
86	Unidentified	–	–	–	25.9/5.0	–	–
87	Ran-specific GTPase-activating protein	RANG_MOUSE	P34022	23.6/5.2	26.4/5.1	26	80
88	Actin, cytoplasmic 1	ACTB_MOUSE	P60710	41.7/5.3	25.8/5.4	20	110
89	Proteasome subunit alpha type 5	PSA5_MOUSE	Q9Z2U1	26.4/4.7	24.3/4.8	15.77[a]	3[b]
90	ATP synthase beta chain, mitochondrial [Precursor]	ATPB_MOUSE	P56480	56.3/5.2	23.9/5.1	15.69[a]	5[b]
91	Rho GDP-dissociation inhibitor 1	GDIR_MOUSE	Q99PT1	23.4/5.1	23.4/5.1	36	155
92	Unidentified	–	–	–	22.8/5.2	–	–
93	Prohibitin	PHB_MOUSE	P67778	29.8/5.6	22.8/5.3	28.31[a]	6[b]
94	Translationally controlled tumour protein	TCTP_MOUSE	P63028	19.5/4.8	22.2/4.9	33	83
95	Unidentified	–	–	–	22.0/4.9	–	–

Table 1. Continued

ID	Protein name	Swiss-Prot entry name	Swiss-Prot accession no.	Calculated MW Da ($\times10^3$)/p*I*	Observed MW Da ($\times10^3$)/p*I*	Sequence coverage %	MASCOT Score
96	Unidentified	–	–	–	22.2/5.1	–	–
97	Lactoylglutathione lyase	LGUL_MOUSE	Q9CPU0	20.7/5.3	22.1/5.1	28	113
98	Prohibitin	PHB_MOUSE	P67778	29.8/5.6	21.2/4.9	46.69[a]	14[b]
99	Unidentified	–	–	–	21.4/5.1	–	–
100	Phosphatidylethanolamine-binding protein	PEBP_MOUSE	P70296	20.7/5.2	21.4/5.1	22	71
101	Unidentified	–	–	–	21.8/5.5	–	–
102	Unidentified	–	–	–	20.3/5.4	–	–
103	S-phase kinase-associated protein 1A	SKP1_MOUSE	Q9WTX5	18.5/4.4	19.2/4.5	23.31[a]	3[b]
104	Unidentified	–	–	–	18.9/4.5	–	–
105	Unidentified	–	–	–	18.0/4.0	–	–
106	Eukaryotic translation initiation factor 5A	IF5A_MOUSE	P63242	16.7/5.1	18.0/5.1	32	82
107	Unidentified	–	–	–	17.7/5.1	–	–
108	Myosin light polypeptide 6	MYL6_MOUSE	Q60605	16.8/4.6	17.1/4.5	47	106
109	Unidentified	–	–	–	17.1/5.0	–	–
110	Unidentified	–	–	–	15.4/4.0	–	–
111	Unidentified	–	–	–	14.3/4.8	–	–
112	Mitochondrial import inner membrane translocase subunit TIM8 A	TIM8A_MOUSE	Q9WVA2	11.0/5.1	14.4/5.0	34.02[a]	3[b]
113	Unidentified	–	–	–	14.6/5.0	–	–
114	Cytochrome c oxidase polypeptide Va, mitochondrial [Precursor]	COX5A_MOUSE	P12787	16.0/6.1	14.5/5.1	17.93[a]	3[b]
115	Unidentified	–	–	–	18.3/5.6	–	–
116	Superoxide dismutase [Cu-Zn]	SODC_MOUSE	P08228	15.8/6.0	17.4/5.6	38.96[a]	5[b]
117	Heat shock-related 70 kD protein 2	HSP72_MOUSE	P17156	69.7/5.6	14.9/5.6	3.79[a]	2[b]
118	Unidentified	–	–	–	16.9/5.7	–	–
119	Superoxide dismutase [Cu-Zn]	SODC_MOUSE	P08228	15.8/6.0	17.4/6.0	39	82
120	Histidine triad nucleotide-binding protein 1	HINT1_MOUSE	P70349	13.6/6.4	15.2/6.3	23.81[a]	4[b]
121	40S ribosomal protein S12	RS12_MOUSE	P63323	14.4/7.0	15.5/6.5	44	70
122	Unidentified	–	–	–	12.7/7.5	–	–
123	Unidentified	–	–	–	13.5/8.1	–	–
124	Profilin I	PROF1_MOUSE	P62962	14.8/8.5	14.9/8.5	68	143
125	Nucleoside diphosphate kinase A	NDKA_MOUSE	P15532	17.2/6.8	17.4/6.6	53	119
126	Unidentified	–	–	–	17.2/7.7	–	–
127	Peptidyl-prolyl cis-trans isomerase A	PPIA_MOUSE	P17742	17.8/7.9	17.8/6.6	30.49[a]	8[b]
128	Unidentified	–	–	–	17.5/6.7	–	–
129	Nucleoside diphosphate kinase B	NDKB_MOUSE	Q01768	17.4/7.0	18.3/7.3	69	135
130	Peptidyl-prolyl cis-trans isomerase A	PPIA_MOUSE	P17742	17.8/7.9	18.0/7.7	52	126
131	Peptidyl-prolyl cis-trans isomerase A	PPIA_MOUSE	P17742	17.8/7.9	17.8/8.0	53	133
132	Cofilin, non-muscle isoform	COF1_MOUSE	P18760	18.4/8.3	18.5/8.2	46	128
133	Cofilin, non-muscle isoform	COF1_MOUSE	P18760	18.4/8.3	18.5/8.5	30	73
134	Unidentified	–	–	–	18.6/6.0	–	–
135	Zfp472 protein	Q8R5B3_MOUSE	Q8R5B3	59.3/8.7	19.5/7.3	22	70
136	Transgelin 2	Q91VU2_MOUSE	Q91VU2	22.4/8.4	21.2/8.4	63	113
137	UMP-CMP kinase	KCY_MOUSE	Q9DBP5	22.2/5.7	21.9/5.6	16.33[a]	3[b]
138	Adenine phosphoribosyltransferase	APT_MOUSE	P08030	19.7/6.3	21.9/5.9	61	142
139	mitochondrial ribosomal protein L15, full insert sequence [Fragment]	Q9CRH4_MOUSE	Q9CRH4	34.9/10.3	21.9/5.9	24	69
140	GrpE protein homolog 1, mitochondrial [Precursor]	GRPE1_MOUSE	Q99LP6	24.3/8.6	21.5/5.9	37	82
141	Unidentified	–	–	–	22.3/6.9	–	–
142	Superoxide dismutase [Mn], mitochondrial [Precursor]	SODM_MOUSE	P09671	24.6/8.8	22.2/7.8	40	95
143	Peroxiredoxin 1	PRDX1_MOUSE	P35700	22.2/8.3	22.2/8.3	50	133
144	Peroxiredoxin 1	PRDX1_MOUSE	P35700	22.2/8.3	22.2/8.5	44	172
145	Unidentified	–	–	–	22.5/5.8	–	–

Table 1. Continued

ID	Protein name	Swiss-Prot entry name	Swiss-Prot accession no.	Calculated MW Da ($\times 10^3$)/pI	Observed MW Da ($\times 10^3$)/pI	Sequence coverage %	MASCOT Score
146	Unidentified	–	–	–	22.4/6.1	–	–
147	Heterogeneous nuclear ribonucleoprotein H	HNRH1_MOUSE	O35737	49.1/5.9	22.8/6.3	21	84
148	Proteasome subunit alpha type 2	PSA2_MOUSE	P49722	25.8/8.4	23.0/6.7	29	64
149	GTP-binding nuclear protein Ran	RAN_MOUSE	P62827	24.4/7.0	22.4/7.0	53	164
150	GTP-binding nuclear protein Ran	RAN_MOUSE	P62827	24.4/7.0	22.6/7.4	23.61[a]	6[b]
151	Peroxiredoxin 6	PRDX6_MOUSE	O08709	24.7/5.7	24.9/5.7	55	121
152	Unidentified	–	–	–	25.2/5.9	–	–
153	Heat-shock protein beta-1	HSPB1_MOUSE	P14602	23.0/6.1	25.0/6.0	47	169
154	Proteasome subunit alpha type 6	PSA6_MOUSE	Q9QUM9	27.4/6.4	25.9/6.2	47	102
155	Protein C14orf166 homolog	CN166_MOUSE	Q9CQE8	28.2/6.4	25.0/6.4	52.87[a]	15[b]
156	Alpha enolase	ENOA_MOUSE	P17182	47.0/6.4	25.5/6.7	17.74[a]	6[b]
157	Triosephosphate isomerase	TPIS_MOUSE	P17751	26.6/7.1	25.0/6.7	45.78[a]	9[b]
158	Triosephosphate isomerase	TPIS_MOUSE	P17751	26.6/7.1	25.1/7.4	34	151
159	High mobility group protein 2	HMG2_MOUSE	P30681	24.0/7.1	24.7/7.8	12.92[a]	2[b]
160	Proteasome subunit beta type 7 [Precursor]	PSB7_MOUSE	P70195	29.9/8.1	27.4/5.9	15	90
161	Endoplasmic reticulum protein ERp29 [Precursor]	ERP29_MOUSE	P57759	28.8/5.9	26.9/6.0	26	91
162	Phosphoglycerate mutase 1	PGAM1_MOUSE	Q9DBJ1	28.7/6.8	26.8/6.7	32	89
163	Adenylate kinase isoenzyme 2, mitochondrial	KAD2_MOUSE	Q9WTP6	25.5/7.2	27.0/7.6	46	84
164	Heat shock cognate 71-kDa protein	HSP7C_MOUSE	P63017	70.9/5.4	27.4/8.0	15	100
165	Electron transfer flavoprotein beta-subunit	ETFB_MOUSE	Q9DCW4	27.3/8.6	26.8/8.4	44	113
166	Similar to kynurenine aminotransferase III	–	gi|51761828[c]	45.0/9.9	26.4/8.6	28	113
167	Heat shock cognate 71-kDa protein	HSP7C_MOUSE	P63017	70.9/5.4	27.9/8.6	19	139
168	Protein disulfide isomerase associated 3	Q99LF6_MOUSE	Q99LF6	56.7/5.9	28.4/5.6	11	70
169	Protein disulfide isomerase A3 [Precursor]	PDIA3_MOUSE	P27773	56.6/6.0	29.5/5.6	18.25[a]	9[b]
170	Protein disulfide-isomerase A3 [Precursor]	PDIA3_MOUSE	P27773	56.6/6.0	29.8/5.7	13	98
171	Proteasome subunit alpha type 1	PSA1_MOUSE	Q9R1P4	29.5/6.0	29.8/6.0	22	79
172	Protein C14orf166 homolog	CN166_MOUSE	Q9CQE8	28.2/6.4	28.3/6.2	21.72[a]	4[b]
173	Unidentified	–	–	–	30.4/6.3	–	–
174	Unidentified	–	–	–	31.1/6.9	–	–
175	Guanine nucleotide-binding protein beta subunit 2-like 1	GBLP_MOUSE	P68040	35.1/7.6	30.7/7.0	33	128
176	Unidentified	–	–	–	29.5/7.0	–	–
177	Unidentified	–	–	–	28.8/7.0	–	–
178	Electron transfer flavoprotein alpha-subunit, mitochondrial [Precursor]	ETFA_MOUSE	Q99LC5	35.0/8.6	31.1/7.3	34	124
179	Guanine nucleotide-binding protein beta subunit-like protein 12.3 [Fragment]	Q9CSQ0_MOUSE	Q9CSQ0	31.0/7.7	30.9/7.7	62	203
180	Unidentified	–	–	–	31.2/8.4	–	–
181	Voltage-dependent anion-selective channel protein 1	VDAC1_MOUSE	Q60932	32.4/8.6	30.9/8.7	30	111
182	Unidentified	–	–	–	32.6/5.9	–	–
183	26S proteasome non-ATPase regulatory subunit 14	PSDE_MOUSE	O35593	34.6/6.1	32.0/5.9	22	90
184	Uridine phosphorylase 1	UPP1_MOUSE	P52624	34.1/6.1	31.5/6.2	29	108
185	Heat shock cognate 71-kDa protein	HSP7C_MOUSE	P63017	70.9/5.4	31.7/6.4	13.93[a]	8[b]
186	similar to 3' of D-containing protein [Fragment]	Q8BZS8_MOUSE	Q8BZS8	31.3/8.2	31.8/7.4	33	75
187	L-Lactate dehydrogenase A chain	LDHA_MOUSE	P06151	36.4/7.8	32.2/7.8	32	128
188	Heterogeneous nuclear ribonucleoproteins A2/B1	ROA2_MOUSE	O88569	36.0/8.7	32.4/8.7	23	98
189	Nucleolin	NUCL_MOUSE	P09405	76.6/4.7	33.8/6.3	15	93
190	LIM and SH3 domain protein 1	LASP1_MOUSE	Q61792	30.0/6.6	34.8/6.5	27	81

Table 1. Continued

| ID	Protein name	Swiss-Prot entry name	Swiss-Prot accession no.	Calculated MW Da ($\times 10^3$)/pI	Observed MW Da ($\times 10^3$)/pI	Sequence coverage %	MASCOT Score
191	Transmembrane GTPase MFN1	MFN1_MOUSE	Q811U4	83.7/6.1	34.6/6.6	15	78
192	Aldose reductase	ALDR_MOUSE	P45376	35.6/6.8	33.5/6.7	30	108
193	Unidentified	–	–	–	34.0/7.5	–	–
194	Annexin A2	ANXA2_MOUSE	P07356	38.5/7.5	33.5/8.0	20.71[a]	6[b]
195	Glyceraldehyde 3-phosphate dehydrogenase	G3P_MOUSE	P16858	35.7/8.5	33.3/8.2	22	111
196	Glyceraldehyde 3-phosphate dehydrogenase	G3P_MOUSE	P16858	35.7/8.5	33.4/8.5	27	79
197	Unidentified	–	–	–	37.1/5.7	–	–
198	Apolipoprotein A-IV [Precursor]	APOA4_MOUSE	P06728	45.0/5.4	36.9/6.0	24	71
199	TNF receptor associated factor 5	TRAF5_MOUSE	P70191	61.1/7.7	35.4/6.1	16	63
200	Heat shock cognate 71-kDa protein	HSP7C_MOUSE	P63017	70.9/5.4	35.8/6.3	15	77
201	Alcohol dehydrogenase [NADP+]	AK1A1_MOUSE	Q9JII6	36.5/6.9	35.5/7.1	18	89
202	Heterogeneous nuclear ribonucleoprotein A/B	ROAA_MOUSE	Q99020	30.8/7.7	36.7/7.8	32	119
203	Fructose-bisphosphate aldolase A	ALDOA_MOUSE	P05064	39.2/8.4	37.8/7.9	32	140
204	Fructose-bisphosphate aldolase A	ALDOA_MOUSE	P05064	39.2/8.4	37.6/8.1	31	133
205	Fructose-bisphosphate aldolase A	ALDOA_MOUSE	P05064	39.2/8.4	37.4/8.3	35	178
206	40-kDa peptidyl-prolyl cis-trans isomerase	PPID_MOUSE	Q9CR16	40.6/7.1	37.8/7.4	26	104
207	Alcohol dehydrogenase class III	ADHX_MOUSE	P28474	39.5/7.6	37.9/6.8	24	86
208	Poly(rC)-binding protein 1	PCBP1_MOUSE	P60335	37.5/6.7	37.7/6.7	22	72
209	Mitotic checkpoint protein BUB3	BUB3_MOUSE	Q9WVA3	37.0/6.2	38.2/6.6	41.10[a]	12[b]
210	DnaJ homolog subfamily B member 11 [Precursor]	DNJBB_MOUSE	Q99KV1	40.6/5.9	39.7/6.0	23.18[a]	9[b]
211	Alpha enolase	ENOA_MOUSE	P17182	47.0/6.4	39.7/6.1	21	93
212	Unidentified	–	–	–	39.4/6.2	–	–
213	Unidentified	–	–	–	39.1/6.3	–	–
214	Heterogeneous nuclear ribonucleoprotein A/B	ROAA_MOUSE	Q99020	30.8/7.7	39.5/6.4	33	100
215	Aspartate aminotransferase, cytoplasmic	AATC_MOUSE	P05201	46.1/6.8	39.4/7.1	26	152
216	Aspartate aminotransferase, cytoplasmic	AATC_MOUSE	P05201	46.1/6.8	39.2/7.1	45	270
217	TAR DNA-binding protein-43	TADBP_MOUSE	Q921F2	44.5/6.3	40.7/6.1	24	133
218	TAR DNA-binding protein-43	TADBP_MOUSE	Q921F2	44.5/6.3	42.5/6.1	22	93
219	Unidentified	–	–	–	43.3/6.6	–	–
220	2-Amino-3-ketobutyrate coenzyme A ligase, mitochondrial [Precursor]	KBL_MOUSE	O88986	44.9/6.9	41.1/6.7	20	79
221	Isocitrate dehydrogenase [NADP] cytoplasmic	IDHC_MOUSE	O88844	46.7/6.5	42.5/6.8	42.51[a]	16[b]
222	26S protease regulatory subunit 8	PRS8_MOUSE	P62196	45.6/7.1	45.0/7.1	15	72
223	26S protease regulatory subunit S10B	PRS10_MOUSE	P62334	44.2/7.1	40.4/7.4	31	130
224	Heterogeneous nuclear ribonucleoprotein D0	HNRPD_MOUSE	Q60668	38.4/7.6	42.5/7.8	25	95
225	Unidentified	–	–	–	41.3/7.7	–	–
226	Acyl-CoA dehydrogenase, medium-chain specific, mitochondrial [Precursor]	ACADM_MOUSE	P45952	46.5/8.6	40.6/7.8	18	90
227	Phosphoglycerate kinase 1	PGK1_MOUSE	P09411	44.4/7.5	41.3/8.1	17	75
228	Unidentified	–	–	–	45.9/8.1	–	–
229	Unidentified	–	–	–	48.4/8.6	–	–
230	47-kDa heat shock protein [Precursor]	HSP47_MOUSE	P19324	46.6/8.9	46.3/8.8	35.01[a]	8[b]
231	Antigenic determinant of rec-A protein	Q8K339_MOUSE	Q8K339	44.7/9.1	41.0/8.9	17	64
232	Unidentified	–	–	–	50.5/9.1	–	–
233	Serine protease inhibitor A3F	SPA3F_MOUSE	Q80X76	52.8/4.9	46.0/5.6	6	56
234	T complex protein-10 (Tcp-10b) mRNA. [Fragment]	O35706_MOUSE	O35706	45.3/5.6	47.8/5.7	13	65
235	Ornithine aminotransferase, mitochondrial [Precursor]	OAT_MOUSE	P29758	48.4/6.2	44.2/5.7	25	141
236	Heat shock cognate 71-kDa protein	HSP7C_MOUSE	P63017	70.9/5.4	41.6/5.8	16	104

Table 1. Continued

ID	Protein name	Swiss-Prot entry name	Swiss-Prot accession no.	Calculated MW Da ($\times10^3$)/pI	Observed MW Da ($\times10^3$)/pI	Sequence coverage %	MASCOT Score
237	60-kDa heat shock protein, mitochondrial [Precursor]	CH60_MOUSE	P63038	61.0/5.9	45.9/5.7	20	84
238	Rab GDP dissociation inhibitor beta-2	GDIC_MOUSE	Q61598	50.5/5.9	47.9/5.8	20	97
239	Heat shock cognate 71-kDa protein	HSP7C_MOUSE	P63017	70.9/5.4	50.7/5.8	19	118
240	Heterogeneous nuclear ribonucleoprotein H'	HNRH2_MOUSE	P70333	49.3/5.9	52.7/5.7	25	76
241	Heterogeneous nuclear ribonucleoprotein H	HNRH1_MOUSE	O35737	49.1/5.9	52.6/5.7	44	164
242	Alpha enolase	ENOA_MOUSE	P17182	47.0/6.4	47.5/6.0	30	110
243	Unidentified	–	–	–	46.0/6.0	–	–
244	Protein disulfide isomerase associated 3	Q99LF6_MOUSE	Q99LF6	56.7/5.9	58.8/5.6	17.62[a]	7[b]
245	T-complex protein 1, epsilon subunit	TCPE_MOUSE	P80316	59.6/5.7	60.2/5.6	14	90
246	Protein disulfide-isomerase A3 [Precursor]	PDIA3_MOUSE	P27773	56.6/6.0	58.4/5.7	32	135
247	T-complex protein 1, alpha subunit B	TCPA2_MOUSE	P11983	60.4/5.8	59.2/5.7	21	117
248	Unidentified	–	–	–	56.8/5.9	–	–
249	T-complex protein 1, beta subunit	TCPB_MOUSE	P80314	57.3/6.0	54.5/6.0	32	145
250	3-Phosphoglycerate dehydrogenase	Q8C603_MOUSE	Q8C603	56.6/5.7	56.7/6.1	10	72
251	PRP19/PSO4 homolog	PRP19_MOUSE	Q99KP6	55.2/6.1	55.3/6.2	23	134
252	Uridine 5'-monophosphate synthase	PYR5_MOUSE	P13439	52.3/6.2	53.5/6.2	15	99
253	RuvB-like 1	RUVB1_MOUSE	P60122	50.2/6.0	53.1/6.2	29	135
254	Aldehyde dehydrogenase, mitochondrial [Precursor]	ALDH2_MOUSE	P47738	56.5/7.5	52.0/6.3	22	145
255	Fascin	FSCN1_MOUSE	Q61553	54.3/6.2	53.1/6.4	46.04[a]	23[b]
256	Septin 11	SEP11_MOUSE	Q8C1B7	49.7/6.2	51.7/6.5	42	113
257	Serine hydroxymethyltransferase, cytosolic	GLYC_MOUSE	P50431	52.6/6.5	51.3/6.5	21	115
258	Alpha enolase	ENOA_MOUSE	P17182	47.0/6.4	47.8/6.2	29	126
259	Elongation factor Tu, mitochondrial [Precursor]	EFTU_MOUSE	Q8BFR5	49.9/7.2	43.9/6.4	28	134
260	Proliferation-associated protein 2G4	PA2G4_MOUSE	P50580	43.7/6.4	45.2/6.5	31	166
261	Unidentified	–	–	–	71.6/6.4	–	–
262	Unidentified	–	–	–	65.8/6.3	–	–
263	T-complex protein 1, gamma subunit	TCPG_MOUSE	P80318	60.6/6.3	64.0/6.3	25	150
264	Phosphoenolpyruvate carboxykinase, mitochondrial precursor [GTP]	PPCKM_MOUSE	Q8BH04	70.5/6.9	65.7/6.4	17	119
265	Stress-induced-phosphoprotein 1	STIP1_MOUSE	Q60864	62.6/6.4	61.5/6.4	34	182
266	Bifunctional purine biosynthesis protein PURH	PUR9_MOUSE	Q9CWJ9	64.2/6.3	62.5/6.5	23	115
267	Heterogeneous nuclear ribonucleoprotein L	HNRPL_MOUSE	Q8R081	60.1/6.7	63.2/6.6	19	107
268	Heterogeneous nuclear ribonucleoprotein L	HNRPL_MOUSE	Q8R081	60.1/6.7	63.4/6.7	17	132
269	Heterogeneous nuclear ribonucleoprotein L	HNRPL_MOUSE	Q8R081	60.1/6.7	63.3/6.9	16	118
270	T-complex protein 1, zeta subunit	TCPZ_MOUSE	P80317	57.9/6.7	60.1/6.7	23	127
271	Dihydrolipoyl dehydrogenase, mitochondrial [Precursor]	DLDH_MOUSE	O08749	54.2/8.0	57.1/6.6	14	95
272	Leucine aminopeptidase 3	Q99P44_MOUSE	Q99P44	56.1/7.6	55.9/6.6	19	102
273	Cytosol aminopeptidase	AMPL_MOUSE	Q9CPY7	52.6/6.6	55.6/6.7	18	121
274	Hypothetical protein D10Wsu52e (P55)	Q99LF4_MOUSE	Q99LF4	55.2/6.8	56.5/6.9	24	128
275	Inosine-5'-monophosphate dehydrogenase 2	IMDH2_MOUSE	P24547	55.8/6.8	55.1/6.9	22	90
276	Glutamate dehydrogenase 1, mitochondrial [Precursor]	DHE3_MOUSE	P26443	61.3/8.1	53.0/6.9	13	85
277	Unidentified	–	–	–	54.1/7.2	–	–
278	Succinyl-CoA:3-ketoacid-coenzyme A transferase 1, mitochondrial [Precursor]	SCOT_MOUSE	Q9D0K2	56.0/8.7	55.7/7.4	15.48[a]	3[b]
279	Pyruvate kinase, isozyme M2	KPYM_MOUSE	P52480	57.8/7.4	59.3/7.3	24	121
280	Pyruvate kinase, isozyme M2	KPYM_MOUSE	P52480	57.8/7.4	59.1/7.7	35	130
281	Serine hydroxymethyl transferase 2	Q99K87_MOUSE	Q99K87	55.8/8.7	53.1/8.1	34	237

Table 1. Continued

ID	Protein name	Swiss-Prot entry name	Swiss-Prot accession no.	Calculated MW Da (×10³)/p*I*	Observed MW Da (×10³)/p*I*	Sequence coverage %	MASCOT Score
282	ATP synthase alpha chain, mitochondrial [Precursor]	ATPA_MOUSE	Q03265	59.8/9.2	53.4/8.2	32	190
283	Far upstream element binding protein 1	FUBP1_MOUSE	Q91WJ8	68.5/7.7	70.7/6.9	10	83
284	Far upstream element binding protein 1	FUBP1_MOUSE	Q91WJ8	68.5/7.7	71.1/7.4	16	102
285	Transketolase	TKT_MOUSE	P40142	67.6/7.2	65.0/7.6	26	198
286	Unidentified	–	–	–	68.8/7.9	–	–
287	Mitogen-activated protein kinase 11	MK11_MOUSE	Q9WUI1	41.4/5.5	64.9/8.3	28	81
288	Heat shock protein 75-kDa, mitochondrial [Precursor]	TRAP1_MOUSE	Q9CQN1	80.2/6.3	71.0/5.7	17	135
289	Glycerol-3-phosphate dehydrogenase, mitochondrial [Precursor]	GPDM_MOUSE	Q64521	80.9/6.2	69.4/5.9	14	69
290	Mitochondrial inner membrane protein	IMMT_MOUSE	Q8CAQ8	83.9/6.2	77.2/5.8	13	88
291	Ezrin	EZRI_MOUSE	P26040	69.3/5.8	74.9/5.8	21	124
292	Far upstream element binding protein 1	FUBP1_MOUSE	Q91WJ8	74.2/6.4	76.9/6.6	20	96
293	DEAD-box protein 3, X-chromosomal	DDX3X_MOUSE	Q62167	73.0/6.7	73.5/6.7	27	192
294	Far upstream element binding protein 1	FUBP1_MOUSE	Q91WJ8	74.2/6.4	76.7/6.9	18	145
295	Aconitate hydratase, mitochondrial [Precursor]	ACON_MOUSE	Q99KI0	85.5/8.1	77.2/7.8	23	137
296	ATP-dependent metalloprotease YME1L1	YMEL1_MOUSE	O88967	80.0/9.0	73.5/8.5	11	71
297	Unidentified	–	–	–	87.3/6.1	–	–
298	Trifunctional purine biosynthetic protein adenosine-3	PUR2_MOUSE	Q64737	107.4/6.3	92.4/6.4	11	95
299	Elongation factor 2	EF2_MOUSE	P58252	95.2/6.4	86.9/6.7	13	112
300	Unidentified	–	–	–	88.4/6.9	–	–

a) Coverage by MS/MS.
b) Number of peptides identified by MS/MS.
c) Entry number from NCBI database.
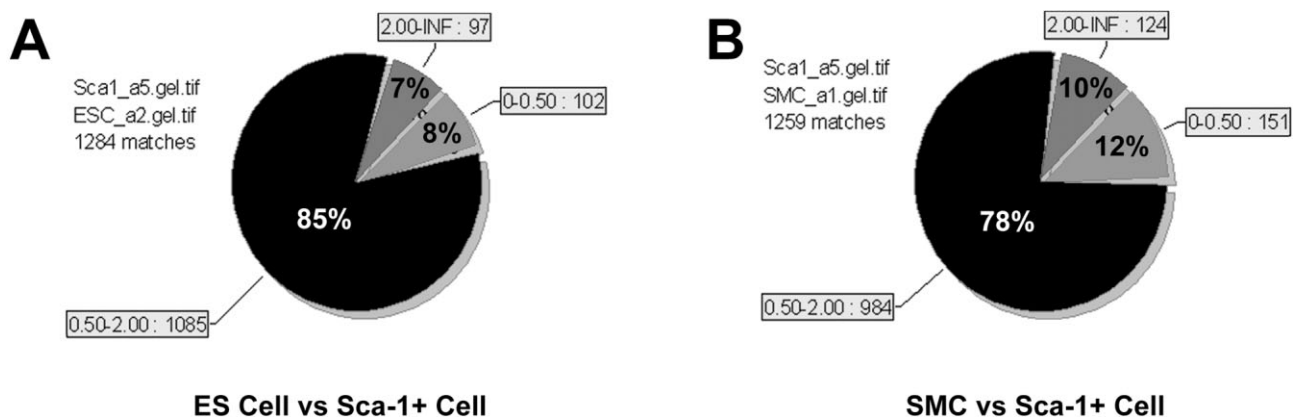
Figure 4. Percentage of differentially expressed spots in Sca-1^{+} progenitor cell gels compared with ES cell gels and SMC gels. 2-DE gel images from Sca-1^{+} progenitor cells, ES cells and SMCs were imported into the ProteomWeaver software (Definiens). Average gels were created from four single gels per group. Pie charts show the percentage of protein spots with twofold increased and decreased protein expression between Sca-1^{+} progenitor cells and ES cells (A) and between Sca-1^{+} progenitor cells and SMCs (B).

So far, we have characterised the protein profile of Sca-1^{+} progenitor cells and mouse arterial SMC. We are currently performing experiments using the DIGE approach to reliably quantify differences in protein expression during stem cell differentiation to SMCs, which should give us further insights into the functional role of the identified proteins.

5 References

[1] Yurugi-Kobayashi, T., Itoh, H., Yamashita, J., Yamahara, K. *et al.*, *Blood* 2003, *101*, 2675–2678.

[2] Doetschman, T. C., Eistetter, H., Katz, M., Schmidt, W., Kemler, R., *J. Embryol. Exp. Morphol.* 1985, *87*, 27–45.

[3] Risau, W., Sariola, H., Zerwes, H. G., Sasse, J. *et al.*, *Development* 1988, *102*, 471–478.

[4] Drab, M., Haller, H., Bychkov, R., Erdmann, B. *et al.*, *FASEB J.* 1997, *11*, 905–915.

[5] Rohwedel, J., Maltsev, V., Bober, E., Arnold, H. H. *et al.*, *Dev. Biol.* 1994, *164*, 87–101.

[6] Bain, G., Kitchens, D., Yao, M., Huettner, J. E., Gottlieb, D. I., *Dev. Biol.* 1995, *168*, 342–357.

[7] Brustle, O., Jones, K. N., Learish, R. D., Karram, K. *et al.*, *Science* 1999, *285*, 754–756.

[8] Soria, B., Roche, E., Berna, G., Leon-Quinto, T. *et al.*, *Diabetes* 2000, *49*, 157–162.

[9] Dani, C., Smith, A. G., Dessolin, S., Leroy, P. *et al.*, *J. Cell Sci.* 1997, *110 (Pt 11)*, 1279–1285.

[10] Poliard, A., Nifuji, A., Lamblin, D., Plee, E. *et al.*, *J. Cell Biol.* 1995, *130*, 1461–1472.

[11] Yamane, T., Hayashi, S., Mizoguchi, M., Yamazaki, H., Kunisada, T., *Dev. Dyn.* 1999, *216*, 450–458.

[12] Abe, K., Niwa, H., Iwase, K., Takiguchi, M. *et al.*, *Exp. Cell Res.* 1996, *229*, 27–34.

[13] Keller, G. M., *Curr. Opin. Cell Biol.* 1995, *7*, 862–869.

[14] Asahara, T., Murohara, T., Sullivan, A., Silver, M. *et al.*, *Science* 1997, *275*, 964–967.

[15] Rafii, S., *J. Clin. Invest.* 2000, *105*, 17–19.

[16] Simper, D., Stalboerger, P. G., Panetta, C. J., Wang, S., Caplice, N. M., *Circulation* 2002, *106*, 1199–1204.

[17] Sata, M., *Trends Cardiovasc. Med.* 2003, *13*, 249–253.

[18] Hill, J. M., Zalos, G., Halcox, J. P., Schenke, W. H. *et al.*, *N. Engl. J. Med.* 2003, *348*, 593–600.

[19] Szmitko, P. E., Fedak, P. W., Weisel, R. D., Stewart, D. J. *et al.*, *Circulation* 2003, *107*, 3093–3100.

[20] Rauscher, F. M., Goldschmidt-Clermont, P. J., Davis, B. H., Wang, T. *et al.*, *Circulation* 2003, *108*, 457–463.

[21] Vasa, M., Fichtlscherer, S., Adler, K., Aicher, A. *et al.*, *Circulation* 2001, *103*, 2885–2890.

[22] Assmus, B., Schachinger, V., Teupe, C., Britten, M. *et al.*, *Circulation* 2002, *106*, 3009–3017.

[23] Hu, Y., Davison, F., Ludewig, B., Erdel, M. *et al.*, *Circulation* 2002, *106*, 1834–1839.

[24] Hu, Y., Davison, F., Zhang, Z., Xu, Q., *Circulation* 2003, *108*, 3122–3127.

[25] Xu, Q., Zhang, Z., Davison, F., Hu, Y., *Circ. Res.* 2003, *93*, e76–86.

[26] Yamashita, J., Itoh, H., Hirashima, M., Ogawa, M. *et al.*, *Nature* 2000, *408*, 92–96.

[27] Sone, M., Itoh, H., Yamashita, J., Yurugi-Kobayashi, T. *et al.*, *Circulation* 2003, *107*, 2085–2088.

[28] Hu, Y., Zhang, Z., Torsney, E., Afzal, A. R. *et al.*, *J. Clin. Invest.* 2004, *113*, 1258–1265.

[29] Vittet, D., Prandini, M. H., Berthier, R., Schweitzer, A. *et al.*, *Blood* 1996, *88*, 3424–3431.

[30] Dunn, M. J., *Methods Mol. Biol.* 1997, *64*, 25–36.

[31] McGregor, E., Kempster, L., Wait, R., Welson, S. Y. *et al.*, *Proteomics* 2001, *1*, 1405–1414.

[32] Yan, J. X., Wait, R., Berkelman, T., Harry, R. A. *et al.*, *Electrophoresis* 2000, *21*, 3666–3672.

[33] Shevchenko, A., Wilm, M., Vorm, O., Mann, M., *Anal. Chem.* 1996, *68*, 850–858.

[34] Perkins, D. N., Pappin, D. J., Creasy, D. M., Cottrell, J. S., *Electrophoresis* 1999, *20*, 3551–3567.

[35] Wilm, M., Shevchenko, A., Houthaeve, T., Breit, S. *et al.*, *Nature* 1996, *379*, 466–469.

[36] Mayr, U., Mayr, M., Yin, X., Begum, S. *et al.*, *Proteomics* 2005, *5*, DOI 10.1002/pmic.200402045.

[37] Elliott, S. T., Crider, D. G., Garnham, C. P., Boheler, K. R., Van Eyk, J. E., *Proteomics* 2004, *4*, 3813–3832.

[38] Mayr, M., Siow, R., Chung, Y. L., Mayr, U. *et al.*, *Circ. Res.* 2004, *94*, e87–96.